PHYSICAL REVIEW B **67**, 100502(R) (2003)

Supercurrent-induced Peltier-like effect in superconductor/normal-metal weak links

Tero T. Heikkilä,[1,2,*] Tommy Vänskä,[1] and Frank K. Wilhelm[3]
[1]*Materials Physics Laboratory, Helsinki University of Technology, P.O. Box 2200, FIN-02015 HUT, Finland*
[2]*Low Temperature Laboratory, Helsinki University of Technology, P.O. Box 2200, FIN-02015 HUT, Finland*
[3]*Sektion Physik and CeNS, Ludwig-Maximilians-Universität, Theresienstrasse 37, D-80333 München, Germany*
(Received 30 October 2002; published 17 March 2003)

The local nonequilibrium quasiparticle distribution function in a normal-metal wire depends on the applied voltage over the wire and the type and strength of different scattering mechanisms. We show that in a setup with superconducting reservoirs, in which the supercurrent and the dissipative current flow (anti) parallel, the distribution function can also be tuned by applying a supercurrent between the contacts. Unlike the usual control by voltage or temperature, this leads to a Peltier-like effect: the supercurrent converts an externally applied voltage into a difference in the effective temperature between two parts of the system maintained at the same potential. We suggest an experimental setup for probing this phenomenon and mapping out the controlled distribution function.

DOI: 10.1103/PhysRevB.67.100502 PACS number(s): 74.25.Fy, 74.40.+k, 74.50.+r, 74.45.+c

Many of the well-understood phenomena in mesoscopic physics can be probed within the linear response of a physical system to an applied external perturbation, i.e., they are governed by equilibrium physics. Recently the attention has turned more towards the study of effects far from equilibrium. The quasiparticle distribution function $f(x;E)$ characterizing the nonequilibrium was measured in a normal-metal (N) wire between two large reservoirs[1,2] through a superconducting (S) tunnel probe. This yielded useful information on the residual interactions between the Fermi-liquid quasiparticles. This nonequilibrium distribution was used to control the supercurrent in a normal-metal weak link.[3–5] Both of these setups serve as different types of local probes for $f(x;E)$.

As a further step, we describe the control of $f(x;E)$ via the supercurrent. We show that, unlike other control parameters, it changes the profile of the effective temperature through the sample in the form of a large Peltier effect, i.e., heating the electrons in one part of the structure, and cooling them in another—even in the case of complete electron-hole symmetry. Moreover, we show how the two types of measurements for $f(x;E)$ can be combined within the same sample.

We concentrate on studying a diffusive normal-metal wire where elastic scattering is the dominant scattering mechanism. In the absence of superconductivity and for wires much shorter than the inelastic scattering length, the steady-state distribution function between two reservoirs with chemical potentials μ_1 and μ_2 has a double-step form, interpolating between the two Fermi functions in the reservoirs.[1]

When the N reservoirs are replaced by superconducting ones, the leading transport mechanism at energies below the superconducting gap Δ is Andreev reflection.[6] This leads to a penetration of superconducting correlations into the N wire (superconducting proximity effect). It modifies the charge and energy conductivities and we may introduce the corresponding diffusion coefficients $\mathcal{D}_T(x;E)$ and $\mathcal{D}_L(x;E)$ depending on space and energy.[7] More importantly, the proximity effect allows supercurrents to flow through the N wire. To describe these effects, it is convenient to separate $f(x;E)$ into symmetric and antisymmetric parts relative to the chemical potential μ_S of the superconductor,

$$f_T(E)\equiv 1-f(\mu_S-E)-f(\mu_S+E), \tag{1}$$

$$f_L(E)\equiv f(\mu_S-E)-f(\mu_S+E). \tag{2}$$

Below, we choose $\mu_S=0$. These functions describe charge and energy distributions, respectively. They satisfy the kinetic equations[7,8]

$$\frac{\partial j_T}{\partial x}=0,\quad j_T\equiv\mathcal{D}_T(x)\frac{\partial f_T}{\partial x}+j_E f_L+\mathcal{T}(x)\partial_x f_L; \tag{3}$$

$$\frac{\partial j_L}{\partial x}=0,\quad j_L\equiv\mathcal{D}_L(x)\frac{\partial f_L}{\partial x}+j_E f_T-\mathcal{T}(x)\partial_x f_T. \tag{4}$$

Here we assume no energy relaxation, so the kinetic equations describe the conservation of $j_T(E)$ and Ej_L, the spectral charge and energy currents, respectively. Terms $\mathcal{D}_T$, $\mathcal{D}_L$, j_E, and $\mathcal{T}$ can be found from quasiclassical equations for the retarded Green's function in the diffusive limit.[9,7] All of them depend on the phase difference ϕ between the superconductors such that for $\phi=0$, j_E and $\mathcal{T}$ vanish. In our case, the charge diffusion coefficient $\mathcal{D}_T$ is increased at most up to 20% from its normal-state value $\mathcal{D}_T=1$,[10] whereas for energies below Δ, $\mathcal{D}_L$ tends towards zero near the S interface, effectively prohibiting energy transport. The term $\mathcal{T}(x;E,\phi)$ (Ref. 8) is obtained as a cross term from the retarded and advanced Green's functions. In general, it is much smaller than the other coefficients. The supercurrent is described by a spectrum $j_E(E;\phi)$ of supercurrent-carrying states,[11–13] which yields a contribution $j_E f_L(x)$ to the spectral charge current and, under nonequilibrium conditions involving $f_T(x)\neq 0$, a contribution to the energy current $Ej_E f_T(x)$.

These kinetic equations have to be supplied with boundary conditions. At N reservoirs, electrons are simply transmitted and the distributions have to match Fermi functions with shifted chemical potentials. At the NS interface for $|E|<\Delta$, Andreev reflection prohibits the transfer of energy into S yielding $j_L=0$. The charge distribution is continuous, which leads to $f_T(E)=0$ at the *NS* interface assuming that there is no charge imbalance in the leads.

The nonequilibrium distribution function may be characterized through its moments, the local chemical potential $\mu(x)$ and the local effective temperature $T_{\rm eff}(x)$. The previous characterizes the charge distribution function as $\mu(x) = \int_0^\infty dE f_T(x;E)$. The effective temperature describes the amount of heat in the electron system and is related to the energy distribution function via

$$\frac{e^2\mathcal{L}_0}{2}T_{\rm eff}^2(x)=\int_0^\infty dE E[f_{L,0}(x;E)-f_L(x;E)], \qquad (5)$$

where $\mathcal{L}_0=(\pi^2 k_B^2/3e^2)$ is the Lorenz number and the corresponding zero-temperature distribution has a step-function form $f_{L,0}(x;E\geqslant 0)=1-\theta[E-\mu(x)]$.

In the absence of the supercurrent, the kinetic Eqs. (3) and (4) are not coupled and, consequently, there is no thermoelectric coupling between the applied voltage and the energy currents. This results from the assumption of bands with complete electron-hole symmetry in the derivation of the formalism. Beyond the limits of the formalism, it is known that electron-hole symmetry breaking leads to small thermoelectric effects in normal metals, limited by the tiny factor k_BT/ϵ_F.[14]

Below, we study a multiterminal setup depicted in the inset of Fig. 2: varying the voltage between the *N* and *S* reservoirs while maintaining the superconductors at equal potentials allows one to vary the distribution function in the phase-coherent wire. Such a device has already been implemented for controlling the critical current for the dc Josephson effect.[5] It permits to study the supercurrent under nonequilibrium conditions without the complications caused by the ac Josephson effect and is, hence, an appropriate system for demonstrating the physics outlined above: As the energy flow $Ej_Ef_T(x)$ carried by the extra quasiparticles injected into the supercurrent-carrying states cannot pass into the superconductors, it has to be counterbalanced by another energy flow. This flow is driven by the gradient of the energy distribution function $E\mathcal{D}_L\partial_x f_L$ and hence, the applied control voltage is converted into a gradient of the effective temperature through the supercurrent.

Solving Eqs. (3) and (4) for $\phi=0$ and $E<\Delta$ is similar to a two-probe *N-S* case:[7] f_L stays constant throughout the phase-coherent wire at its value in the *N* reservoir, $f_L^0(V) = (\tanh[(E+eV)/2k_BT]+\tanh[(E-eV)/2k_BT])/2$ and f_T is slightly modified from the linear space dependence due to the proximity effect on $\mathcal{D}_T$.[10] Increasing the phase ϕ induces a finite supercurrent into the weak link, thereby coupling f_L and f_T. First neglecting the small coefficient $\mathcal{T}$, we get

$$\frac{\partial f_L}{\partial x}=-j_E\frac{f_T}{\mathcal{D}_L},\quad \frac{\partial}{\partial x}\left(\mathcal{D}_T\frac{\partial f_T}{\partial x}\right)=j_E^2\frac{f_T}{\mathcal{D}_L}. \qquad (6)$$

Assuming that j_E is small, we observe that the major change due to the supercurrent is expected for $f_L(E,x)$; in particularly, it will depend on space.

In general, a closed-form solution for $f_L(x;E)$, $f_T(x;E)$ cannot be found. Therefore, we focus on a numerical solu-

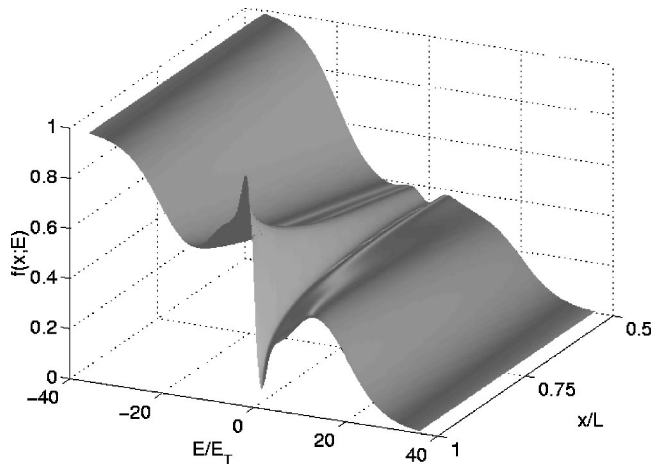

FIG. 1. Quasiparticle distribution function $f(x;E)$ in the right-horizontal arm for voltage $V=20E_T/e$, temperature $T=4E_T/k_B$, and phase difference $\phi=\pi/2$ between the superconductors. The large deviations from the rounded staircase form are created by the supercurrent flowing in the structure.

tion of both the spectral and kinetic equations. Here and below, we assume that all the energies are below Δ. The effect of the supercurrent on the distribution functions is clearest at a low temperature $k_BT\lesssim E_T$. The resulting distribution function $f(x,E)$ for the right-hand horizontal arm is plotted in Fig. 1 for $\phi=\pi/2$, yielding a supercurrent close to its maximum. As expected, the antisymmetric part of $f(x;E)$ has become space dependent, its energy dependence following that of j_E. Fixing a position in space, chosen, for example, near the *NS* interface in the left-hand side horizontal arm, allows us to observe how the distribution function changes as a function of phase ϕ, i.e., as it is driven by the supercurrent. This is illustrated in Fig. 2, where $f_L(E;\phi)$ is plotted for a few values of ϕ.

In the three-probe case, the chemical potential $\mu(x)$ interpolates nearly linearily between the chemical potentials of the superconductor and the normal reservoir and varies only little with the supercurrent. The changes in the effective temperature $T_{\rm eff}$ are much more pronounced. In the absence of the supercurrent, $T_{\rm eff}$ is

$$T_{\rm eff}^0\equiv T_{\rm eff}(\phi=0)=\sqrt{T^2+\{V^2-(\mu(x)/e)^2\}/\mathcal{L}_0}. \qquad (7)$$

Both $T_{\rm eff}(x;\phi=0)$ and $\mu(x;\phi=0)$ are symmetric in the two horizontal arms. The supercurrent-induced change in $f_L(x;E)$ can be described through the change of the effective temperature compared to Eq. (7), such that $T_{\rm eff}(x) = [T_{\rm eff}^0(x)^2+S(x;V)+\delta\mu(x;\phi)]^{1/2}$, where

$$S(x;V)=\frac{6}{\pi^2k_B^2}\int_0^\infty dE E[f_L^0(E;V)-f_L(x;E)] \qquad (8)$$

and $\delta\mu(x;\phi)\equiv[\mu(x;\phi)^2-\mu(x;\phi=0)^2]/2$ describes the change in the local chemical potential due to the supercurrent, a much smaller term than $S(x)$. The kinetic equations imply that the supercurrent-induced change of the distribution function f_L is antisymmetric between the two arms, hence so is $S(x)$, i.e., $T_{\rm eff}$ increases in one arm and decreases

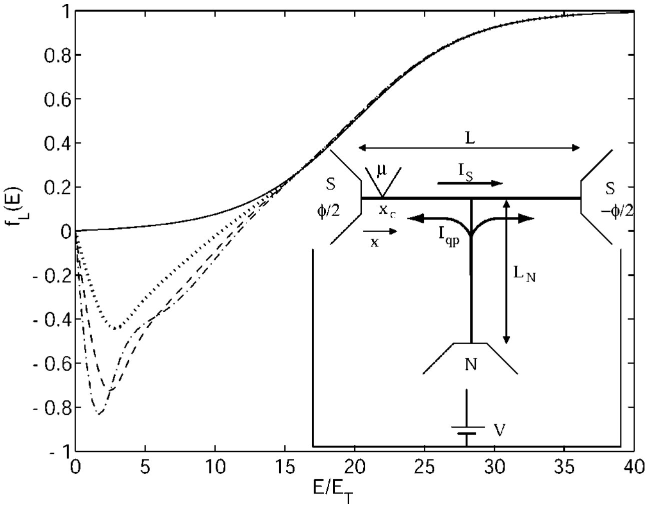

FIG. 2. Supercurrent-driven distribution function $f_L(E)$ at the left NS interface as a function of energy for $\phi=0$ (solid), $\phi=0.12\pi$ (dotted), $\phi=0.24\pi$ (dashed), and $\phi=\pi/2$ (dash dotted). The result is obtained with $T=4E_T/k_B$ and $V=20E_T/e$. The corresponding changes of f_L by the supercurrent in the right arm have the opposite sign. Inset: the system under consideration. We assume symmetric horizontal wires of length $L/2$. This length defines the Thouless energy of the weak link, $E_T\equiv\hbar D/L^2$. The resistance of the weak link is $R_{\rm w}$ and of the vertical wire $R_{\rm c}$. Measurement of the predicted effects can be performed by placing a superconducting tunnel probe at position $x=x_c$, near the NS interface.

in the other one. Hence, the system works analogously to a Peltier device, where the control current is replaced by the supercurrent: the supercurrent "cools" one part of the system, transferring the heat to another part. The supercurrent-induced temperature change $S(x;V)$ is illustrated in Fig. 3.

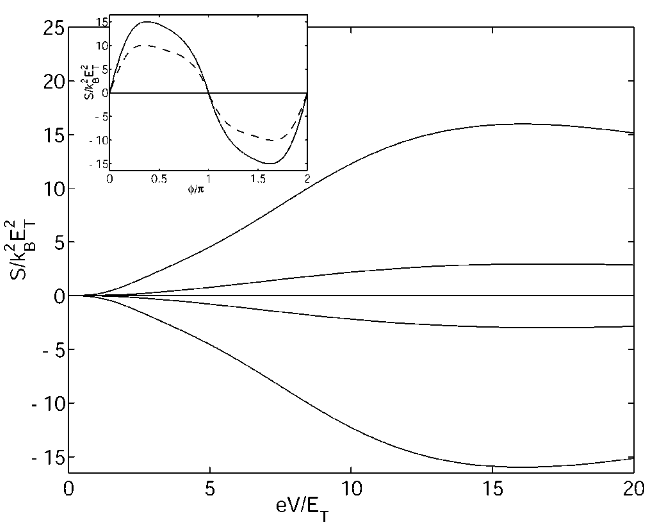

FIG. 3. Supercurrent-induced change $S(x;V)$ in the effective temperature as a function of voltage eV/E_T at different positions in the weak link with $\phi=\pi/2$. From top to bottom: $x=0$, $x=L/4$, $x=L/2$, $x=3L/4$, and $x=L$. Here $x=0$ and $x=L$ correspond to the left and right S interfaces and $x=L/2$ to the crossing point. Inset shows the phase dependence of $S(x=0)$ for $eV=12E_T$ (solid) and $eV=8E_T$ (dashed). In both curves, the bath temperature $T=0$.

To obtain an estimate for $S(x;V,\phi)$, we approximate $\mathcal{D}_T(E;x)=1$ and find

$$S=\frac{2E_T^2R_{\rm w}}{L^2(R_{\rm w}+R_{\rm c})}\int_0^\infty dEEj_E(E)f_T^0(E)\int_x^{L/2}\frac{x'dx'}{\mathcal{D}_L(x';E)}. \tag{9}$$

At low temperatures $k_BT\ll eV$, f_T reduces to a step function around the potential eV in the reservoir, cutting the integration off at $E=eV$. Thus, this current-induced temperature change, which is similar to the Peltier effect, is much larger than in conventional single-metal setups.

For the measurement of the predicted effects in the distribution function, we suggest a setup shown in the inset of Fig. 2–very similar to those used in Refs. 1,2. Such a setup has also been used as a local thermometer[15] of the electronic temperatures. A superconducting wire is connected to the horizontal arm via a highly resistive tunneling layer (I) at position, say, $x=x_c$. The dc current is then given by the tunneling quasiparticle current

$$I_J=\frac{1}{eR}\int_{-\infty}^{\infty}dE\rho_S(E+\mu)\rho(E)[f_0(E+\mu)-f(E)], \tag{10}$$

where $N_S\rho_S(E)$ is the BCS density of states (DOS) of the tunnel probe, $N_N\rho(E)$ is the local DOS in the mesoscopic wire at $x=x_c$, N_S and N_N are the normal-state DOS's for the two materials at $E=E_F$, $f_0(E)$ is the Fermi function, and $f(E)$ is the distribution function to be measured. When all the wires are in the normal state, the resistance through the tunnel junction is R. We can separate this expression as $I_J=I_1+I_2$, where I_1 is the tunneling current for the equilibrium system $V=0$, probing $\rho(E)$ and

$$I_2=\frac{1}{eR}\int_0^\infty dE\rho(E)\{f_T(E)[\rho_S(\mu+E)+\rho_S(\mu-E)] +[f_L(E)-\tanh(E/2k_BT)][\rho_S(\mu+E)-\rho_S(\mu-E)]\} \tag{11}$$

depends on the state of the wire, and for an equilibrium state, $V=0$, vanishes. In order to isolate I_2, one can first determine I_1 as a function of the supercurrent by investigating the equilibrium case. Then, I_1 may be substracted from the nonequilibrium results, leaving only currents I_2. Moreover, $I_2(\mu)+I_2(-\mu)$ is proportional to the first part of Eq. (11), dependent on $f_T(E)$, and $I_2(\mu)-I_2(-\mu)$ to the second, dependent on $f_L(E)$.

With the above setup, the distribution functions may be characterized as a function of both the voltage V and the supercurrent driven through the weak link. The setup also makes it possible to measure the local distribution function both through the NIS contact and through the SNS critical current. These two independent probes should permit to distinguish the contributions from different inelastic scattering effects along the lines of Ref. 1.

So far we have completely neglected inelastic scattering in the wires. We can include energy relaxation due to electron-electron scattering phenomenologically, generalizing the method of Ref. 16 to include the effect of supercurrent. In the limit $L \gg l_\varepsilon$, we may describe the nonequilibrium distribution functions by Fermi functions with local chemical potential and temperature. In this case, assuming for simplicity $\mathcal{D}_T=1$ and $\mathcal{T}=0$, we can integrate the two kinetic equations over energy, obtain kinetic equations for $\mu(x)$ and $T_{\rm eff}(x)$ and find in the limit of high Δ

$$\partial_x^2 \mu(x) = -\partial_x I_S(x), \tag{12}$$

$$e^2 \mathcal{L}_0 \widetilde{T}(x) \partial_x T_{\rm eff}(x) = -\widetilde{\mu}(x) \partial_x \mu(x) + Q_S. \tag{13}$$

Here $I_S(x) = [\int dE j_E(E) f_L(E,x)]/2$ is the local supercurrent, $2\mathcal{L}_0 e^2 \widetilde{T} = -\int {\rm d}EE\mathcal{D}_L \partial_T f_L$ and $2\widetilde{\mu}(x) = -\int dEE\mathcal{D}_L \partial_\mu f_L$ describe the local temperature and chemical potential modified by $\mathcal{D}_L$, respectively, and $Q_S = [\int dEEj_E(E) f_T(E,x)]/2$ is the energy current carried by the nonequilibrium supercurrent. The first equation states the conservation of the total current whereas the latter describes the temperature profile. In the absence of the proximity effect, these yield the effective temperature given in Eq. (7). Similarly as above, the effective temperature can also in this case be tuned via the supercurrent, through the control of Q_S.

The predicted effect resembles a previously studied phenomenon in bulk superconductors,[17] where a temperature gradient along with a supercurrent generates a charge imbalance in *S*. Here, the finite voltage (described through f_T) along with the supercurrent produces a temperature gradient (spatial variation of f_L).[18]

In Ref. 19, another thermoelectric effect, the thermopower, has been measured experimentally in a similar type of a system. The coupling of the distribution functions through the supercurrent may explain part of the observed effects. In Ref. 20, thermopower has been studied in the regime of high tunnel barriers and within linear response, leading also to an unexpectedly large effect. In that paper, all the distribution functions are, besides minor corrections, in quasiequilibrium: the transport is essentially driven by the discontinuities at the tunneling barriers. Moreover, Ref. 21 studies the Andreev interferometers through a numerical scattering approach, and predicts an oscillating thermopower as a function of the phase. However, there the quasiparticle current and supercurrent do not flow in parallel and the magnitude of the effect may be strongly affected by the very small size of the studied structure.

Summarizing, we predict that in a nonequilibrium situation created by applying a voltage between a normal metal and two superconductors, the nonequilibrium distribution functions in the normal-metal wire can be tuned by the supercurrent flowing between the superconductors. This results in a supercurrent-controlled Peltier effect. The predicted effect can be observed by the measurement of the tunneling current from an additional superconductor.

We thank N. Birge for the idea to this work and J. von Delft, D. J. van Harlingen and J. Pekola for suggestions on the manuscript. This work was supported by the Graduate School in Technical Physics at the Helsinki University of Technology.

*Email address: Tero.T.Heikkila@hut.fi

[1] H. Pothier *et al.*, Phys. Rev. Lett. **79**, 3490 (1997).
[2] F. Pierre *et al.*, Phys. Rev. Lett. **86**, 1078 (2001).
[3] J.J.A. Baselmans, A.F. Morpurgo, B.J. van Wees, and T.M. Klapwijk, Nature (London) **397**, 43 (1999).
[4] J.J.A. Baselmans, B.J. van Wees, and T.M. Klapwijk, Phys. Rev. B **63**, 094504 (2001).
[5] J. Huang *et al.*, Phys. Rev. B **66**, 020507(R) (2002).
[6] A.F. Andreev, Zh. Éksp. Teor. Fiz. **46**, 1823 (1964) [JETP **19**, 1228 (1964)].
[7] W. Belzig *et al.*, Superlattices Microstruct. **25**, 1251 (1999).
[8] S.-W. Lee, A.V. Galaktionov, and C.-M. Ryu, J. Korean Phys. Soc. **34**, S193 (1999).
[9] K.D. Usadel, Phys. Rev. Lett. **25**, 507 (1970).
[10] P. Charlat *et al.*, Phys. Rev. Lett. **77**, 4950 (1996). This modification of $\mathcal{D}_T$ can also be tuned by a phase between two superconductors in an Andreev interferometer [P.G.N. de Vegvar, T.A. Fulton, W.H. Mallison, and R.E. Miller, *ibid.* **73**, 1416 (1994)]. This tuning leads to the phase dependence of $\mu(x;\varphi)$.
[11] F.K. Wilhelm, G. Schön, and A.D. Zaikin, Phys. Rev. Lett. **81**, 1682 (1998).
[12] S.K. Yip, Phys. Rev. B **58**, 5803 (1998).
[13] T.T. Heikkilä, J. Särkkä, and F.K. Wilhelm, Phys. Rev. B **66**, 184513 (2002).
[14] N. W. Ashcroft and N. D. Mermin, *Solid State Physics* (Saunders College, Orlando, 1976).
[15] J.M. Rowell and D.C. Tsui, Phys. Rev. B **14**, 2456 (1976).
[16] K.E. Nagaev, Phys. Rev. B **52**, 4740 (1995).
[17] C.J. Pethick and H. Smith, Phys. Rev. Lett. **43**, 640 (1979); J. Clarke, B.R. Fjordbøge, and P.E. Lindelof, *ibid.* **43**, 642 (1979); A. Schmid and G. Schön, *ibid.* **43**, 793 (1979); J. Clarke and M. Tinkham, *ibid.* **44**, 106 (1980).
[18] However, the mechanism for the coupling between the temperature gradient and charge imbalance is different in these two cases: whereas in bulk superconductors, it arises from the superconducting condensate that converts quasiparticle currents into supercurrents, the phenomenon depicted here is due to the energy current carried by the supercurrent in the nonequilibrium state.
[19] J. Eom, C.J. Chien, and V. Chandrasekhar, Phys. Rev. Lett. **81**, 437 (1998).
[20] R. Seviour and A.F. Volkov, Phys. Rev. B **62**, R6116 (2000).
[21] N.R. Claughton and C.J. Lambert, Phys. Rev. B **53**, 6605 (1996).